A study of the variations of oxidation–reduction potential, pH, and dissolved oxygen during photo-Fenton oxidation of methyl tert-butyl ether in the presence of a nanosized zero-valent iron particle, hydrogen peroxide, and ultraviolet radiation

Esmaeil Azizi[a,b,*], Afshin Darsanj[a], Hamidreza Zakeri[c], Mehdi Ghayebzadeh[d], Zeinab Heidaripour[e]

[a]*Department of Environmental Health Engineering, Faculty of Health, Determinants of Research Center of Kermanshah University of Medical Sciences, Kermanshah, Iran, Tel. +98 9143896906; email: azizi.esmaeel@gmail.com (E. Azizi), Tel. +98 9368328239; email: afshin.darsanj1371@gmail.com (A. Darsanj)*
[b]*Water and Wastewater Company of West Azerbaijan Province, Ministry of Energy, Iran*
[c]*Ferdows School of Paramedical and Health, Birjand University of Medical Sciences, Birjand, Iran, Tel. +98 9151602132; email: hrzakeri66@gmail.com (H. Zakeri)*
[d]*Department of Environmental Health Engineering, Health and Environment Research Center, Tabriz University of Medical Sciences, Tabriz, Iran, Tel. +98 9141586994; email: m.ghayebzadeh@gmail.com (M. Ghayebzadeh)*
[e]*Department of Environmental Health Engineering, Research Center of Yasuj University of Medical Sciences, Yasuj, Iran, Tel. +98 9177497046; email: zeinabheidarypour66@yahoo.com (Z. Heidaripour)*

Received 8 October 2019; Accepted 25 April 2020

ABSTRACT

The changes in oxidation–reduction potential (ORP), pH level, and dissolved oxygen (DO) concentration during the redo/oxidative degradation of methyl tert-butyl ether (MTBE) by nanosized zero-valent iron (nZVI) combined with hydrogen peroxide addition and ultra-violate radiation were investigated. The optimal ratio of oxidants depended on the initial concentration of MTBE. For instance, MTBE was completely removed at the 60 min of contact time and with its initial concentration of 0.05 mm MTBE and all nZVI particle/hydrogen peroxide ratios (10:100, 20:200, and 30:300 mg/L). In contrast, 54.2% of MTBE (0.27 mM) remained after 90 min of contact time when its initial concentration was 0.5 mM and the nZVI/hydrogen peroxide ratio was 10:100 mg/L. It was observed during the oxidation process the pH was increased from 4 to 7 and DO was decreased from 9 to 0 mg/L. Significant fluctuation of ORP was observed over the oxidation time. According to results, the initial dose of oxidants can significantly affect the pH levels and DO concentrations of effluent, and ORPs. It can be concluded that in order to achieve the higher removal rate by the nZVI/photo-Fenton process, it is vital to adjust the values of pH, DO, and oxidation–reduction at optimal ranges.

Keywords: Nano zero valent iron (nZVI); Photo-Fenton; Methyl tert-butyl ether; Dissolved oxygen; Oxidation–reduction potential; pH

1. Introduction

Environmental and water pollution by the emerging and hazardous synthetic organic pollutants has recently become an issue of international concern [1–3]. Methyl tert-butyl ether (MTBE) is one of the organic compounds most commonly used as a gasoline additive to raise the octane number or make gasoline burn cleaner [4,5]. This hazardous
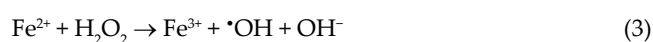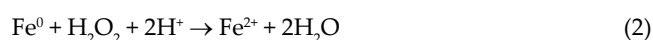
* Corresponding author.

pollutant has been detected in groundwater as a result of gasoline spills or leaking during production, distribution, and storage [6,7]. Since the late 1970s, MTBE has replaced lead (as an anti-knock agent), resulting in the production of a high volume of it. On the other hand, due to its high stability and low biodegradability, its concentration in nature has been increasing over the last decades [8,9]. Low Henry constant, high resistance to biological decomposition, and high water-solubility has resulted in high mobility, unwillingness to stay in the soil, and the sustainability of MTBE in the environment [10,11]. MTBE has relatively high solubility, exhibits lower adsorption to the soil, and is more resistant to chemical degradation. Its water solubility of about 50 g/L makes it approximately 25 times more soluble than benzene and the BTEX (benzene, toluene, ethyl-benzene, and xylene) constituents [12,13]. The most important sources of environmental pollution by MTBE are gas supply stations, gas transfer, and storage activities [14]. MTBE has been categorized by the International Agency for Research on Cancer (IARC) as a possible cancer-causing compound in humans in the C-group of carcinogenic compounds [15]. The US Environmental Protection Agency (U.S. EPA) has recommended a limit of MTBE in drinking water at 20–40 μg/L based on the smell and taste threshold. The range reported by the EPA is about 20,000–100,000 times lower than the range observed for rodent carcinogenicity symptoms. EPA has banned the addition of MTBE to US gas since May 2006 due to its very low smell threshold [16]. The low volatility of MTBE in water (10 times lower than benzene) leads to inefficient removal of MTBE by air stripping process from water [17]. On the other hand, due to its complex chemical structure ($C_5H_{12}O$), MTBE has been known as a resistant compound to biological degradation in aqueous solutions [18]. In search of practical methods for the degradation of the MTBE in aqueous solutions, several methods of advanced oxidation technologies have reportedly achieved promising results. Advanced oxidation processes (AOPs) are considered as promising methods for the oxidation of pathogens, organic, and inorganic pollutants due to the generation of free hydroxyl radicals in aqueous environments [19–21]. AOPs generate the high oxidative power hydroxyl radical to degradation of refractory compounds in queues solutions [22,23]. In an ideal AOP, organic compounds eventually turn into water and carbon dioxide [14,24]. It has been reported that AOPs are significantly effective for the removal of various concentrations of MTBE (0.1–1 mg/L) from aqueous solutions, compared to other physical and biological processes [7,25]. Zero-valent metals have been recently introduced as an effective reductant, being a possible source of iron in the Fenton oxidation process for the treatment of contaminated water [26,27]. Compared to other metals, the zero-valent iron (ZVI) and nano-sized particles of zero-valent iron (nZVI) are more abundant, cheaper, non-toxic, more active, and effective for the removal of pollutants [28–31]. nZVI has been considered as an active metal and effective reducing agent with high oxidation–reduction potential (ORP) ($E^0 = 0.44$ V) [32].
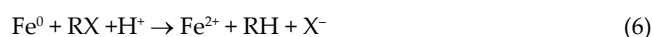
It has been reported that nZVI is effective for the elimination and/or dichlorination of some hazardous organic compounds (e.g., chlorine organic compounds) [33], reduction of organic compounds by conversion of nitrate to ammonia in acidic conditions [34,35], and conversion of toxic and hazardous compounds to less toxic compounds in zero-order reactions and under acidic pH conditions [36].

The mechanism of decomposition of contaminants by nZVI involves the direct transfer of electrons from nZVI to the pollutant that convert the pollutant into non-toxic or less toxic compounds [37]. In addition, nZVI has the potential to oxidize and decompose pollutants in the presence of soluble oxygen as a result of transferring two electrons to the O_2 molecule and the production of hydrogen peroxide (H_2O_2) [Eq. (1)]. The H_2O_2 generated during this process can be reduced to the water molecule by transferring two other electrons from the nZVI [Eq. (2)]. Moreover, the combination of H_2O_2 and Fe^{2+} (Fenton process) leads to the production of hydroxyl radical ($^\bullet$OH) which is one of the most effective agents for the oxidation of organic compounds in water [Eq. (3)] [38,39].

$$Fe^0 + O_2 + 2H^+ \rightarrow Fe^{2+} + H_2O_2 \tag{1}$$

$$Fe^0 + H_2O_2 + 2H^+ \rightarrow Fe^{2+} + 2H_2O \tag{2}$$

$$Fe^{2+} + H_2O_2 \rightarrow Fe^{3+} + {}^\bullet OH + OH^- \tag{3}$$

The high reduction potential of nZVI makes the function desirable. During this process, the oxidized iron [Eq. (4)] and the alkyl aldehydes [Eq. (5)] can be reduced. The final equation of the process under optimal thermodynamic conditions will be favorable [Eq. (6)] [40].

$$Fe^0 \rightarrow Fe^{2+} + 2e^- \tag{4}$$

$$RX + 2e^- + H^+ \rightarrow RH + X^- \tag{5}$$

$$Fe^0 + RX + H^+ \rightarrow Fe^{2+} + RH + X^- \tag{6}$$

nZVI also produces hydrogen gas and hydroxide ions in reaction with H_2O_2, which leads to an increase in pH level of the solution [Eq. (7)] [41].

$$Fe^0 + 2H_2O \rightarrow Fe^{2+} + 2OH^- + H_2 \tag{7}$$
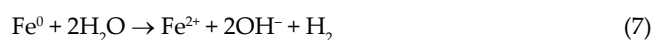
Similar to the Fenton oxidation process, the addition of nZVI to H_2O_2 can result in the generation of $^\bullet$OH and subsequently more degradation of organic pollutants. However, one of the major advantages of using nZVI compared to the conventional Fenton process is the use of solid iron nanoparticles as the Fe^{2+} source instead of soluble iron sulfate ($FeSO_4$) [42]. The reason is that the application of iron sulfate as a source of Fe^{2+} leads to the release of sulfate ions (SO_4^{2-}) in the solution. The generation of SO_4^{2-} in the solution decreases the process efficiency due to the formation of strong complexes between both Fe(II) and Fe(III) ions and SO_4^{2-}, which affect the distribution and reactivity of the iron species presented in the solution [43,44]. It has been reported that the application of nZVI does not lead to the generation of SO_4^{2-} [44]. In the conventional Fenton process, the application of soluble iron increases the consumption of chemicals and the production of relatively high amounts of

iron-rich sludge [45,46]. On the other hand, the complexity and reactivity of the nZVI-Fenton process are more than the conventional Fenton process due to the high reactive surface area that consequently can provide a higher density of reactive sites for the reduction of metals and subsequently higher production of hydroxyl radicals and removal potential of nZVI [46,47]. Therefore, continuous monitoring of parameters in the process is vital to maintaining optimal conditions [48].

Both ORP and dissolved oxygen (DO) are considered as two important parameters to operate the biological and chemical wastewater treatment processes [49]. The addition of nZVI to aqueous solutions containing organic compounds can reduce the DO of the solution, due to the high reduction potential of nZVI [50]. However, nZVI reduces ORP by DO consumption. In addition, the chemical reaction of nZVI with organic compounds can result in the consumption of hydrogen ion and consequently, it will lead to the increment of the pH level [46]. Therefore, measurement of these three parameters (DO, ORP, and pH) can be considered as an effective tool to evaluate the performance of nZVI-Fenton AOPs. In previous studies the variations of ORP, DO, and pH have been monitored during the oxidation reactions with probes in batch systems [46,51]. It has been reported that measurement of ORP, DO, and pH parameters during an nZVI-Fenton process for the removal of azo-dye [46] and chromium (VI) [51] from wastewater can contribute to the reliable evaluation of the efficiency of the process. However, the performance evaluation of the AOP for the removal of organic contaminants from water in the presence of ultra-violate (UV), H_2O_2, and nZVI using the three parameters of DO, ORP, and pH has been rarely studied in the literature.

The advantages of using UV irradiation combined with other oxidants in order to enhance the efficiency of MTBE oxidation were shown in many previous studies [43,52]. Also, degradation of MTBE was investigated by other methods such as anodic Fenton treatment [53]. But more recently the vacuum ultraviolet (VUV) irradiation was studied as a novel method in the advanced oxidation of organics [54,55]. The VUV-based AOPs have some advantages such as the modular apparatus and the homogeneity of the treatment, which has shown effectiveness towards the degradation of compounds over the simple oxidation [55]. In the present study, UV light was used as long as chemical oxidants including H_2O_2 and nZVI. The UV irradiation was used because of its possible potential to enhance the generation of $^\bullet$OH radicals and consequently improve the pollutant removal. It should be noted that as well as the nature of oxidants, the chemical structure of pollutants can impact the three mentioned parameters during the chemical oxidation processes and consequently the efficiency of pollutant removal. Therefore, the main objective of the present study was performance evaluation of the UV/nZVI/H_2O_2 process based on the measurement of selected parameters including pH, DO, and ORP for the removal of MTBE from aqueous solution. The main objectives of this study were (1) to investigate the efficiency of UV/nZVI/H_2O_2 on MTBE degradation as a AOPs treatment system, and (2) to study on ORP, pH, and DO variations during the oxidation time.

2. Materials and methods

2.1. Experimental set-up and materials

The schematic diagram of the experimental set-up used for the oxidation of MTBE by the UV/nZVI/H_2O_2 process is presented in Fig. 1. The cubic oxidation reactor was made of Plexiglas with a capacity of 1 L. In order to adjust the temperature of the oxidation environment, the reactor was equipped with a cooling jacket. The cool water was circulated in the cooling jacket to fix the reaction temperature between 24°C and 26°C. A medium-pressure mercury-vapor lamp with a radiation intensity of 19.5 wm^{-2} was used as the source of UV radiation. The lamp was embedded in the middle of the reactor by the quartz glass cylinder. The outer wall of the reactor was coated with a thin foil laminate not only to maintain the UV rays in the reactor but also to prevent the exposure of users to the UV light. Moreover, a circulator water pump was used to ensure the complete mixing and uniformity of the solution inside the reactor during the process (Fig. 1).

H_2O_2 with a purity of 30% (laboratory grade) was used to prepare different concentrations of 10, 20, and 30 mg/L of H_2O_2 in the solutions. The purity of methyl tertiary butyl ether $((CH_3)_3COCH_3)$ was 99.9%. Other chemical compounds such as n-pentane, toluene, Hydrogen chloride (HCl), and sodium hydroxide (NaOH) were used for the synthesis of nZVI and pH adjustment. All chemicals were supplied by Merck Company, Inc.

2.2. Synthesis of nZVI

There are various methods for the synthesis of iron nanoparticles [56–58]. The iron nanoparticles used in this
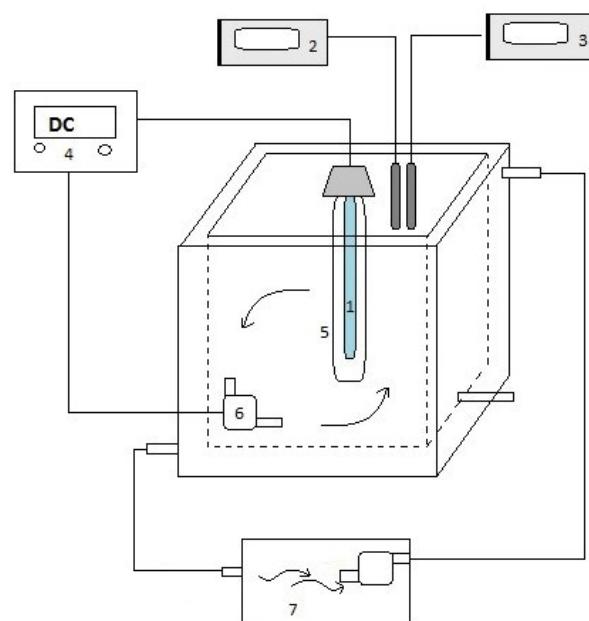

Fig. 1. Schematic diagram of the experimental set-up used for oxidation of MTBE by UV/nZVI/H_2O_2. (1) UV lamp, (2) ORP and pH meter, (3) DO meter, (4) electrical source, (5) quartz cell, (6) circulator pump, (7) cooling water circulator system.

study were synthesized by the sodium borohydride method [59,60]. One of the most important advantages of this method is its ease of use. According to the previous studies [61–63], in order to synthesize nZVI with the borohydride method, the nanoparticles were synthesized by the addition of 0.1 molar sodium borohydride solution to a ferric chloride solution ($FeCl_3 \cdot 6H_2O$) at the ambient temperature. The 0.02 molar of ferric chloride solution was prepared by adding 0.5406 g of $FeCl_3 \cdot 6H_2O$ in 100 mL of water–ethanol solution with a volumetric ratio of 1/4.

2.3. Fenton oxidation process

Synthetic solutions were prepared at different concentrations of MTBE. Synthesized nZVI particles and H_2O_2 were added to the reaction solution and the UV lamp was turned on at the beginning of the photo-Fenton oxidation process.

The contact time of each oxidation process was 90 min and the sampling process was conducted at specifically selected time intervals. After extraction of MTBE by (e.g., liquid–liquid extraction method), extracts were immediately injected to the gas chromatography (GC) device to measure the concentration of MTBE. The values of pH, ORP, and DO parameters were simultaneously measured during the process by the installed probes in the reactor.

2.4. Analytical methods

The concentrations of MTBE were measured by the gas chromatograph (0.25 mm × 60 m, J&W DB-624 GC-5890) equipped with a flame ionization detector (FID). The injection port temperature was set at 180°C. The oven temperature was set to 50°C and ramped to 200°C at 50°C/min. The detector temperature was 200°C. Helium gas was used as a carrier gas. The scanning electron microscopy technique (SEM) was used to determine the properties of the synthesized iron nanoparticles.

3. Results and discussion

3.1. Analysis of prepared nZVI by TEM and SEM

According to the SEM image as it can be observed in Fig. 2a, the particle size of synthesized granular Fe^0 was less than 100 nm in diameter. The measured diameter indicates increases of available surface area and therefore the chemical reactivity of nZVI particles. This observation was in agreement with previous studies of nZVI synthesis by the sodium borohydride method [51].

In addition, the TEM image (Fig. 2b) represents the presence of the core and shell layers of nZVI particles. The central regions of nZVI particles that have a darker color than the outer regions are the particle core, and the lighter color represents the shell of nZVI. The core is formed of zero-valent metallic iron and the shell is formed of iron oxides. These results are in good agreement with previous studies [47,59].

3.2. nZVI/H₂O₂ concentration and MTBE removal

The oxidation of MTBE at different initial concentrations of 0.05, 0.1, 0.25, and 0.5 mM (mmol/L) and in the presence of different doses of H_2O_2/nZVI ratios (10:100, 20:200, and 30:300 mg/L), during a 90 min oxidation period was evaluated. In order to prepare the Fenton solution, the ratio of 1/10 of H_2O_2/nZVI was used.

Since acidic pH levels (3–5) have been found to be suitable for the Fenton oxidation process [64,65], the initial pH of the solution was adjusted to 4. As it is shown in Fig. 3, at the constant concentration of oxidants, the amount of MTBE removal was decreased over oxidation time by increasing the initial concentration of MTBE from 0.05 to 0.5 mm.

It can be attributed to the sufficient hydroxyl radicals presented for oxidizing MTBE throughout the process at lower concentrations of MTBE. However, increasing the concentration of MTBE resulted in complete consumption of all remained hydroxyl radicals which can make process suffer from the lack of enough oxidants and consequently reduced the oxidization rate of both MTBE and its intermediate compounds. The correlation of initial concentration of MTBE and its removal efficiency at a constant concentration of oxidants has also been reported in the literature [9,60,63].

In contrast, the increase of H_2O_2/nZVI concentration (i.e., 10:100, 20:200, and 30:300 mg/L) led to an incensement in MTBE removal due to the generation of more hydroxyl radicals. According to Eq. (3), the chemical reaction between nZVI and H_2O_2 yields the production of $^\bullet$OH. Meanwhile, H_2O_2 can absorb energy from UV irradiation leading to the production of $^\bullet$OH. So, increasing the initial oxidant
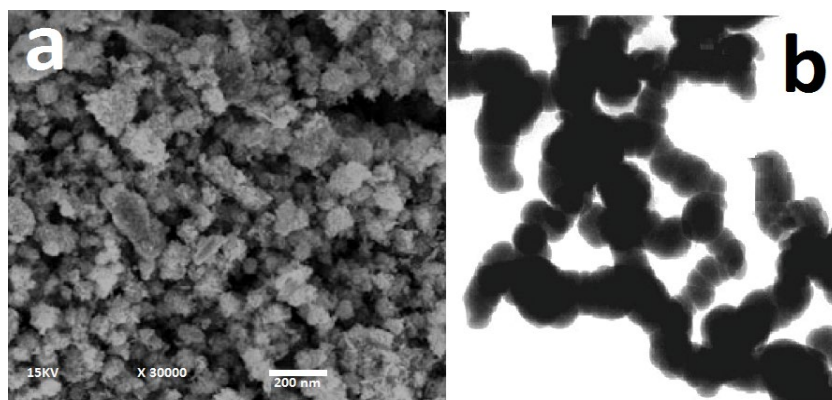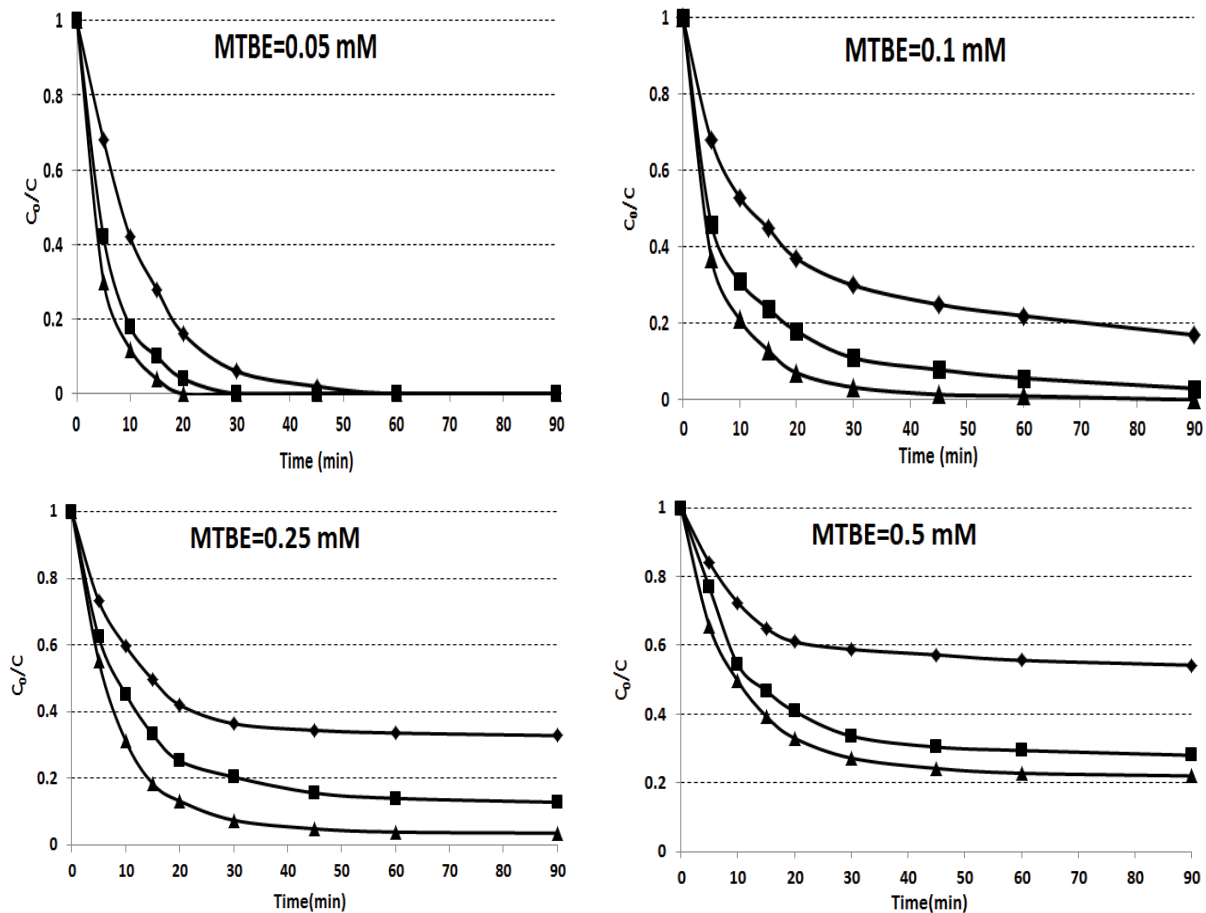

Fig. 2. (a) SEM and (b) TEM images of synthesized nZVI.

Fig. 3. Variation of MTBE concentration (C_0/C) per time in different initial concentrations of MTBE (0.05, 0.25, 0.1, and 0.5 mM) in different oxidant dose H_2O_2/nZVI (10:100◆, 20:200■, and 30:300▲).

concentration will increase the energy absorption and production of more $^\bullet$OH [9]. Therefore, the normalized amount of remained MTBE (C/C_0) in the reaction solution depends on its initial concentrations.

The $^\bullet$OH radicals produced by H_2O_2/nZVI/UV remove the MTBE by simultaneous decomposition mechanisms of the chemical bonds of organic pollutant and generation of Fe^{+2} ions [66]. It has been observed that in low initial concentrations of MTBE because of the efficiency of oxidation is significantly high due to the presence of adequate oxidant agents such as $^\bullet$OH in the solution. For instance, MTBE with an influent concentration of 0.05 mM was completely removed under 90 min of reaction time and all Fenton doses. In contrast, similar observation only took place at 30:300 mg/L of H_2O_2/nZVI for the initial concentrations of 0.1 mM of MTBE.

According to the results, it can be concluded that the oxidation efficiency strongly depends on the amount of $^\bullet$OH produced inside the reactor. So that at the first 30 min of oxidation time, the high removal rate of MTBE was observed due to the presence of a high concentration of $^\bullet$OH. The continuous reduction of MTBE concentration during the oxidation process indicates the continuous production of Fe^{2+} from the residual Fe^0 nanoparticles in the reactor (Eq. (1)). The produced Fe^{2+} can be converted to the Fe^{3+} through the

reaction by the H_2O_2. This can lead to the enhancement of pH level due to the generation of OH^- which is the other product of reaction [Eq. (3)].

According to Fig. 3, increasing the H_2O_2/nZVI doses led to the removal of higher concentrations of MTBE. However, the observed improvement of the MTBE removal was not equal at different ratios of H_2O_2/nZVI. When the oxidizing dosage of H_2O_2/nZVI changed from 10:100 to 20:200, the oxidation efficacy of MTBE significantly increased. However, the final concentration of MTBE in the solution was slightly different in H_2O_2/nZVI doses of 30:300 and 20:200. Therefore, it can be argued that the optimal point, known as optimal dose ratio, is a relative concentration of H_2O_2/nZVI and MTBE which achieves the highest removal of MTBE in the shortest time and the lowest dose of the chemicals. In this study, the ratio of 20:200 was found to be the optimal oxidation ratio for the studied MTBE concentrations which can achieve up to 100% of MTBE removal.

3.3. Changes of pH, ORP, and DO

3.3.1. Changes of pH during the process

According to reactions (1)–(3), the production of hydroxyl radical during the nZVI/H_2O_2 oxidation process caused the
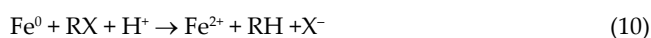
oxidation of organic compounds. At high amounts of nZVI (e.g., 300 mg/L), the production of Fe^{2+} can lead to the increase of the hydroxyl radical production. In addition, according to these reactions, the generated OH^- can increase the pH level of the solution during the oxidation process. The increase in the pH level enhances the reaction of Fe^{+3} ions with OH^- which led to the formation and subsequently precipitation of $Fe(OH)_2$ and $Fe(OH)_3$ [Eqs. (8) and (9)]. Therefore, this can prove the low dissolution of the soluble iron at high pH levels.

$$Fe^{2+} + 2OH^- \rightarrow Fe(OH)_2\downarrow \tag{8}$$

$$4Fe(OH)_2 + 2H_2O + O_2 \rightarrow 4Fe(OH)_3\downarrow \tag{9}$$
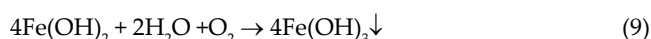
As shown in Fig. 4a, the pH of the solution slowly increased by the addition of H_2O_2/nZVI at the beginning of the oxidation process. The reason is related to the consumption of 2 moles of H^+ during the reaction between nZVI and H_2O_2 [Eq. (2)] as well as the production of OH^- derived from the ferrite ion reaction in the presence of H_2O_2 [Eq. (4)]. It was found out that the rate of pH increase strongly depends on the oxidizing agent dose. The results indicated that the pH of the solution increased from 4 up to higher than 8 in the H_2O_2/nZVI ratio of 30:300 after 30 min of reaction time. It can indicate the considerable amount of produced OH^- and consequently the formation of high amounts of hydroxyl radicals. This phenomenon was not considerable at oxidants doses less than 30:300. However, when the pH reached the basic range, it caused the oxidation of Fe^{2+} with OH^- and the generation of $Fe(OH)_2$. According to Eq. (8), both the consumption of hydroxide ions and the decrease of oxidant concentrations reduced the rate of OH^- production during oxidation. Therefore, it resulted in reducing the pH of the solution toward a neutral pH range (Fig. 4a).

3.3.2. Changes of DO during the process

In general, the addition of nZVI causes DO to be reduced by the following reactions:

$$Fe^0 + RX + H^+ \rightarrow Fe^{2+} + RH + X^- \tag{10}$$

$$2Fe^0 + 2H_2O + O_2 \rightarrow 2Fe^{2+} + 4OH^- \tag{11}$$

$$2Fe^{2+} + 2H_2O \rightarrow 2Fe^{3+} + H_2 + 2OH^- \tag{12}$$

According to Eq. (10), reduction of iron enhances the consumption of hydrogen ions, which Fe^0 nanoparticles react with DO in Eq. (11), and releases hydroxyl radicals. As can be observed, the reaction of nZVI oxidation with DO leads to the production of Fe^{2+} after the addition of nZVI to the solution. The produced Fe^{2+} from the nZVI oxidation was used in another reaction to produce Fe^{3+}. The generated OH^- during reaction leads to an increase in the pH level of the solution. The increased rate of pH was directly related to the amount of nZVI. For instance, 2 mol OH^- was generated from each mole of nZVI [Eq. (12)].

It was found that the reduction of DO in the solution was dependent on the initial concentrations of oxidants.

For instance, the DO concentration of the solution dropped almost to zero in the oxidizing ratio of 30:300 after about 20 min from the beginning of the oxidation reaction. In contrast, the concentration of DO was stable at about 1.5 mg/L in the oxidizing ratio of 10:100 even at 90 min of reaction time.

According to the previous studies, the amount of DO rapidly decreased at the beginning of the oxidation process by the addition of nZVI to the solution. However, in some reports, the amount of DO was slowly increased which may be contributed to the effect of surface aeration phenomena [49,56]. However, this can only occur when the surface of reaction solution is in contact with the air.

In the present study, an insignificant increase of the DO level after the loss of oxygen concentration in the final stages of oxidation was observed due to the improper isolation of the reactor and the limited amount of air contacted with the reaction solution. DO in aqueous solutions is a common oxidizing agent that can accept electrons. In the conventional nZVI process, DO can be consumed by the generated electrons from the corrosion of nZVI in water. Therefore, the concentration of DO decreased rapidly. This phenomenon occurred due to the application of high amounts of nZVI or the prolongation of the oxidation process (Fig. 4b). In cases where the air is injected into the oxidation system, the oxygen concentration recovered due to the continuous presence of DO in the reaction solution. Therefore, oxygen always acted as an oxidizing agent for the oxidation of nZVI, and subsequently the oxidation of ferric hydroxide ($Fe(OH)_2$). Therefore, the pH of the reaction solution increased due to the production of OH^-.

3.3.3. Changes of ORP during the process

In a Fenton process, both oxidation and reduction reactions are involved. Therefore, the ORP of the reaction medium can change during Fenton-based oxidation reactions. ORP is one of the most important factors affecting the overall oxidation process. Since variations in ORP values affect both the concentration of the DO and the production and consumption of OH^- and H^+, it can also cause a variation in the pH of the solution [67].

The ORP value decreased abruptly after the addition of nZVI due to the high reduction potential of nZVI (–0.440 V) (Eq. (13)). The higher dose of the nZVI will lead to a more negative ORP [48].

$$Fe^{2+} + 2e^- \rightarrow Fe_{(s)} \qquad E^0 = -0.440 \text{ V} \tag{13}$$

However, it was observed that the ORP rapidly increased to a positive value by the addition of hydrogen peroxide to the solution. The reason for this observation was correlated to the high oxidizing potential of H_2O_2 which caused the generation of hydroxyl radicals and the formation of precipitations during the oxidation reaction. In the present study, it was observed that the value of ORP had high fluctuations during the oxidation process, which was occurred due to the variations in the initial concentrations of oxidants. The most significant change of ORP happened in the initial oxidation ratio of 30:300. As presented in Fig. 4c, the addition of nZVI to the reaction solution at the beginning of the oxidation process, led to a sharp decrease in the ORP
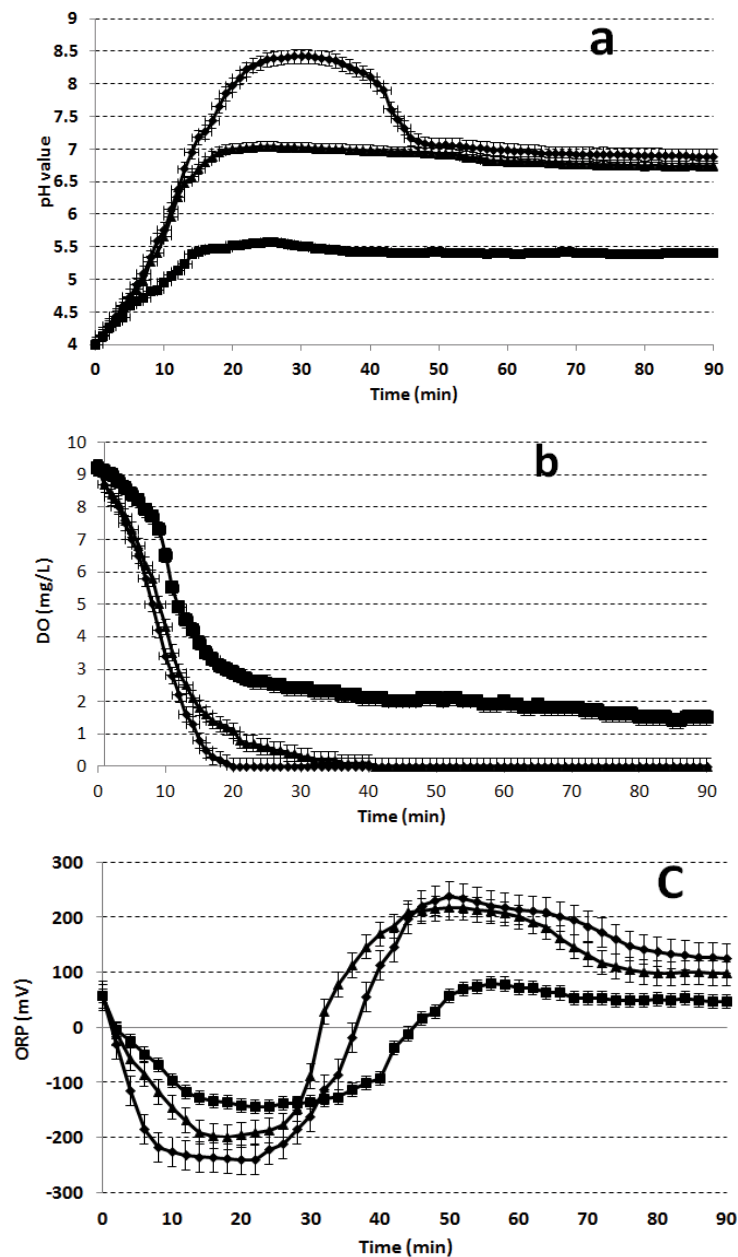
Fig. 4. Variation of (a) pH, (b) DO, and (c) ORP during the MTBE oxidation by UV/nZVI/H$_2$O$_2$ at different oxidant doses (10:100◆, 20:200■, and 30:300▲).

and the domination of strongly negative conditions inside the oxidation reactor. The logic behind that was the rapid oxidation of the nanoparticle surface that occurred at the early stages of the oxidation time. During the process, due to the deposition of iron oxides on the outer surface of the nanoparticles, the role of H$_2$O$_2$ in the liberation of hydroxyl radicals became more considerable and this led to a strong positive ORP in the solution. However, the ORP value of the reaction medium decreased again (Fig. 4c) due to the full consumption of hydrogen peroxide, the low rate of production of hydroxyl radicals as well as the lack of adequate soluble oxygen. Thus, anaerobic conditions were dominated in such a situation.

4. Conclusion

In the present study, the efficacy and performance of UV/nZVI/H$_2$O$_2$ AOP for the removal of MTBE were evaluated by the measurement of variation of pH, DO, and ORP levels during the process. It was observed that the efficiency of MTBE degradation considerably depends on the concentrations of oxidants. At optimal oxidants dosages, the oxidation method can remove up to 100% of MTBE under laboratory conditions and therefore, it can be considered as a promising option. Furthermore, it was observed that the change of pH, DO, and ORP levels depend on the initial concentrations of both oxidant and MTBE. In addition,

the changes in the amount of each of these factors can also affect the rate and extent of oxidation. It can be concluded that it is necessary to adjust the pH, DO, and ORP factors in a suitable range in order to prevent the undesirable effects during $UV/H_2O_2/nZVI$ oxidation process. Therefore, all the selected variables have a critical role in the performance of the applied process and must be considered for efficient removal of MTBE.

Acknowledgments

References

[1] X. Duan, S. Indrawirawan, J. Kang, W. Tian, H. Zhang, X. Duan, X. Zhou, H. Sun, S. Wang, Synergy of carbocatalytic and heat activation of persulfate for evolution of reactive radicals toward metal-free oxidation, Catal. Today., (2019), doi: 10.1016/j. cattod.2019.02.051.

[2] E. Ahmadi, S. Yousefzadeh, M. Ansari, H. Ghaffari A. Azari, M. Miri, A. Mesdaghinia, R. Nabizadeh, B. Kakavandi, P. Ahmdi, M. Badi, M. Gholami, K. Sharafi, M. Karimaei, M. Ghoochani, M. Brahmand, S. Mohseni, M. Sarkhosh, S. Rezaei, H. Asgharnia, E. Dehghanifard, B. Jafari, A. Morte-zapour, V. Moghaddam, M. Mahmoudi, N. Taghipour, Performance, kinetic, and biodegradation pathway evaluation of anaerobic fixed film fixed bed reactor in removing phthalic acid esters from wastewater, Sci. Rep., 7 (2017), doi: 10.1038/srep41020.

[3] S. Yousefzadeh, E. Ahmadi, M. Gholami, H. Ghaffari, A. Azari, M. Ansari, M. Miri, K. Sharafi, S. Rezaei, A comparative study of anaerobic fixed film baffled reactor and up-flow anaerobic fixed film fixed bed reactor for biological removal of diethyl phthalate from wastewater: a performance, kinetic, biogas, and metabolic pathway study, Biotechnol. Biofuels, 10 (2017), doi: 10.1186/s13068-017-0826-9.

[4] M. Mehrjouei, S. Müller, D. Möller, Decomposition kinetics of MTBE, ETBE and, TAEE in water and wastewater using catalytic and photocatalytic ozonation, J. Mol. Catal A: Chem., 386 (2014) 61–68.

[5] A.V. Russo, D.N.D. Lobo, S.E. Jacobo, Removal of MTBE in columns filled with modified natural zeolites, Procedia Mater. Sci., 8 (2015) 375–382.

[6] M. Nousiainen, S. Holopainen, J. Puton, M. Sillanpää, Fast detection of methyl tert-butyl ether from water using solid phase microextraction and ion mobility spectrometry, Talanta, 84 (2011) 738–744.

[7] S.R. Cater, M.I. Stefan, J.R. Bolton, A.S. Amiri, UV/H_2O_2 treatment of methyl tert-butyl ether in contaminated waters, Environ. Sci. Technol. Lett., 34 (2000) 659–662.

[8] M.A. Khan, S.H. Lee, S. Kang, K.J. Paeng, G. Lee, S.E. Oh, B.H. Jeon, Adsorption studies for the removal of methyl tert-butyl ether on various commercially available GACs from an aqueous medium, Sep. Sci. Technol., 46 (2011) 1121–1130.

[9] Q. Hu, C. Zhang, Z. Wang, Y. Chen, K. Mao, X. Zhang, Y. Xiong, M. Zhu, Photodegradation of methyl tert-butyl ether (MTBE) by UV/H_2O_2 and UV/TiO_2, J. Hazard. Mater., 154 (2008) 795–803.

[10] Y. Zhang, F. Jin, Z. Shen, R. Lynch, A. Al-Tabbaa, Kinetic and equilibrium modelling of MTBE (methyl tert-butyl ether) adsorption on ZSM-5 zeolite: batch and column studies, J. Hazard. Mater., 347 (2018) 461–469.

[11] S.G. Huling, S. Ko, S. Park, E. Kan, Persulfate oxidation of MTBE-and chloroform-spent granular activated carbon, J. Hazard. Mater., 192 (2011) 1484–1490.

[12] P.J. Squillace, J.F. Pankow, N.E. Korte, J.S. Zogorski, Review of the environmental behavior and fate of methyl tert-butyl ether, Environ. Toxicol. Chem., 16 (1997) 1836–1844.

[13] D. Zadaka-Amir, A. Nasser, S. Nir, Y.G. Mishael, Removal of methyl tertiary-butyl ether (MTBE) from water by polymer–zeolite composites, Microporous Mesoporous Mater., 151 (2012) 216–222.

[14] I. Levchuk, A. Bhatnagar, M. Sillanpää, Overview of technologies for removal of methyl tert-butyl ether (MTBE) from water, Sci. Total Environ., 476 (2014) 415–433.

[15] W. Hartley, A. Englande, D. Harrington, Health risk assessment of groundwater contaminated with methyl tertiary butyl ether (MTBE), Water Sci. Technol., 39 (1999) 305–310.

[16] N. Kuburovic, M. Todorovic, V. Raicevic, A. Orlovic, L. Jovanovic, J. Nikolic, V. Kuburovic, S. Drmanic, T. Solevic, Removal of methyl tertiary butyl ether from wastewaters using photolytic, photocatalytic and microbiological degradation processes, Desalination, 213 (2007) 123–128.

[17] S. Mohebali, Degradation of methyl t-butyl ether (MTBE) by photochemical process in nanocrystalline TiO_2 slurry: mechanism, by-products and carbonate ion effect, J. Environ. Chem. Eng., 1 (2013) 1070–1078.

[18] M. Mehrjouei, S. Müller, D. Möller, A review on photocatalytic ozonation used for the treatment of water and wastewater, Chem. Eng. J., 263 (2015) 209–219.

[19] A.R. Matin, S. Yousefzadeh, E. Ahmadi, A. Mahvi, M. Alimohammadi, H. Aslani, R. Nabizadeh, A comparative study of the disinfection efficacy of H_2O_2/ferrate and UV/ H_2O_2/ ferrate processes on inactivation of *Bacillus subtilis* spores by response surface methodology for modeling and optimization, Food Chem. Toxicol., 116 (2018) 129–137.

[20] S. Yousefzadeh, R. Nabizadeh, A. Mesdaghinia, S. Nasseri, P. Hezarkhani, M. Beikzadeh, M. Valadi Amin, Evaluation of disinfection efficacy of performic acid (PFA) catalyzed by sulfuric and ascorbic acids tested on *Escherichia coli* (ATCC, 8739), Desal. Water. Treat., 52 (2014) 3280–3289.

[21] A. Shokri, A.H. Joshagani, Using microwave along with TiO_2 for degradation of 4-chloro-2-nitrophenol in aqueous environment, Russ. J. Appl. Chem., 89 (2016) 1985–1990.

[22] A. Shokri, K. Mahanpoor, Degradation of ortho-toluidine from aqueous solution by the TiO_2/O_3 process, Int. J. Ind. Chem., 8 (2017) 101–108.

[23] A. Shokri, The treatment of spent caustic in the wastewater of olefin units by ozonation followed by electrocoagulation process, Desal. Water Treat., 111 (2018) 173–182.

[24] E. Azizi, M. Fazlzadeh, M. Ghayebzadeh, L. Hemati, M. Beikmohammadi, H.R. Ghaffari, H.R. Zakeri, K. Sharafi, Application of advanced oxidation process (H_2O_2/UV) for removal of organic materials from pharmaceutical industry effluent, Environ. Prot. Eng., 43 (2017) 183–191.

[25] V. Augugliaro, M. Litter, L. Palmisano, J. Soria, The combination of heterogeneous photocatalysis with chemical and physical operations: a tool for improving the photoprocess performance, J. Photochem. Photobiol., C, 7 (2006) 127–144.

[26] S. Yousefzadeh, A.R. Matin, E. Ahmadi, Z. Sabeti, M. Alimohammadi, H. Aslani, R. Nabizadeh, Response surface methodology as a tool for modeling and optimization of *Bacillus subtilis* spores inactivation by UV/nano-Fe⁰ process for safe water production, Food Chem. Toxicol., 114 (2018) 334–345.

[27] S. Li, W. Wang, F. Liang, W.X. Zhang, Heavy metal removal using nanoscale zero-valent iron (nZVI): theory and application J. Hazard. Mater., 322 (2017) 163–171.

[28] K.V.G. Ravikumar, S. Santhosh, S.V. Sudakaran, Y.V. Nan-charaiah, P. Mrudula, N. Chandrasekaran, A. Mukherjee, Biogenic nano zero valent iron (Bio-nZVI) anaerobic granules for textile dye removal, J. Environ. Chem. Eng., 6 (2018) 1683–1689.

[29] H. Dong, Q. He, G. Zeng, L. Tang, L. Zhang, Y. Xie, Y. Zeng, F. Zhao, Degradation of trichloroethene by nanoscale zero-valent iron (nZVI) and nZVI activated persulfate in the absence and presence of EDTA, Chem. Eng. J., 316 (2017) 410–418.

[30] H.Y. Shu, M.C. Chang, C.C. Chang, Integration of nanosized zero-valent iron particles addition with UV/H_2O_2 process for purification of azo dye Acid Black 24 solution, J. Hazard. Mater., 167 (2009) 1178–1184.

[31] J. Farrell, M. Kason, N. Melitas, T. Li, Investigation of the long-term performance of zero-valent iron for reductive dechlorination of trichloroethylene, Environ. Sci. Technol., 34 (2000) 514–521.

[32] A.M.E. Khalil, O. Eljamal, B.B. Saha, N. Matsunaga, Performance of nanoscale zero-valent iron in nitrate reduction from water using a laboratory-scale continuous-flow system, Chemosphere, 197 (2018) 502–512.

[33] Y. Zhang, G.B. Douglas, L. Pu, Q. Zhao, Y. Tang, W. Xu, B. Luo, W. Hong, L. Cui, Z. Ye, Zero-valent iron-facilitated reduction of nitrate: chemical kinetics and reaction pathways, Sci. Total Environ., 598 (2017) 1140–1150.

[34] Y. Mu, H.Q. Yu, J.C. Zheng, S.J. Zhang, G.P. Sheng, Reductive degradation of nitrobenzene in aqueous solution by zero-valent iron, Chemosphere, 54 (2004) 789–794.

[35] B. Li, J. Zhu, Removal of p-chloronitrobenzene from groundwater: effectiveness and degradation mechanism of a heterogeneous nanoparticulate zero-valent iron (NZVI)-induced Fenton process, Chem. Eng. J., 255 (2014) 225–232.

[36] R. Li, Y. Gao, X. Jin, Z. Chen, M. Megharaj, R. Naidu, Fenton-like oxidation of 2,4-DCP in aqueous solution using iron-based nanoparticles as the heterogeneous catalyst, J. Colloid Interface Sci., 438 (2015) 87–93.

[37] S.E. Mylon, Q. Sun, T.D. Waite, Process optimization in use of zero valent iron nanoparticles for oxidative transformations, Chemosphere, 81 (2010) 127–131.

[38] M. Eglal, Nanofer Zero-Valent Iron Nanoparticles: Surface Morphology, Structure and Reactivity with Contaminants, Ph.D. Dissertation, Concordia University, 2014.

[39] V. Janda, P. Vasek, J. Bizova, Z. Belohlav, Kinetic models for volatile chlorinated hydrocarbons removal by zero-valent iron, Chemosphere, 54 (2004) 917–925.

[40] H. Zhang, H.J. Choi, C.P. Huang, Treatment of landfill leachate by Fenton's reagent in a continuous stirred tank reactor, J. Hazard. Mater., 136 (2006) 618–623.

[41] L.G. Devi, C. Munikrishnappa, B. Nagaraj, K.E. Rajashekhar, Effect of chloride and sulfate ions on the advanced photo Fenton and modified photo Fenton degradation process of Alizarin Red S, J. Mol. Catal. A: Chem., 374 (2013) 125–131.

[42] M.R. Taha, A. Ibrahim, Characterization of nano zero-valent iron (nZVI) and its application in sono-Fenton process to remove COD in palm oil mill effluent, J. Environ. Chem. Eng., 2 (2014) 1–8.

[43] A.N. Módenes, F.R. Espinoza-Quiñones, F.H. Borba, D.R. Manenti, Performance evaluation of an integrated photo-Fenton – electrocoagulation process applied to pollutant removal from tannery effluent in batch system, Chem. Eng. J., 197 (2012) 1–9.

[44] R.F. Yu, H.W. Chen, W.P. Cheng, Y.J. Lin, C.L. Huang, Monitoring of ORP, pH and DO in heterogeneous Fenton oxidation using nZVI as a catalyst for the treatment of azo-dye textile wastewater, J. Taiwan Inst. Chem. Eng., 45 (2014) 947–954.

[45] D. O'Carroll, B. Sleep, M. Krol, H. Boparai, C. Kocur, Nanoscale zero valent iron and bimetallic particles for contaminated site remediation, Water Resour., 51 (2013) 104–122.

[46] X.Q. Li, D.W. Elliott, W.X. Zhang, Zero-valent iron nanoparticles for abatement of environmental pollutants: materials and engineering aspects, Crit. Rev. Solid State Mater. Sci., 31 (2006) 111–122.

[47] K. Acuna-Askar, A. Englande, C. Hu, G. Jin, Methyl tertiary-butyl ether (MTBE) biodegradation in batch and continuous upflow fixed-biofilm reactors, Water Sci. Technol., 42 (2000) 153–161.

[48] K. Rusevova, F.D. Kopinke, A. Georgi, Nano-sized magnetic iron oxides as catalysts for heterogeneous Fenton-like reactions—influence of Fe(II)/Fe(III) ratio on catalytic performance, J. Hazard. Mater., 241 (2012) 433–440.

[49] R.F. Yu, F.H. Chi, W.P. Cheng, J.C. Chang, Application of pH, ORP, and DO monitoring to evaluate chromium(VI) removal from wastewater by the nanoscale zero-valent iron (nZVI) process, Chem. Eng. J., 255 (2014) 568–576.

[50] B. Vaferi, M. Bahmani, P. Keshavarz, D. Mowla, Experimental and theoretical analysis of the UV/H_2O_2 advanced oxidation processes treating aromatic hydrocarbons and MTBE from contaminated synthetic wastewaters, J. Environ. Chem. Eng., 2 (2014) 1252–1260.

[51] S. Hong, H. Zhang, C.M. Duttweiler, A.T. Lemley, Degradation of methyl tertiary-butyl ether (MTBE) by anodic Fenton treatment, J. Hazard. Mater., 144 (2007) 29–40.

[52] S. Giannakis, I. Hendaoui, M. Jovic, D. Grandjean, L.F. De Alencastro, H. Girault, C. Pulgarin, Solar photo-Fenton and UV/H_2O_2 processes against the antidepressant Venlafaxine in urban wastewaters and human urine. Intermediates formation and biodegradability assessment, Chem. Eng. J., 308 (2017) 492–504.

[53] H. Amanollahi, G. Moussavi, S. Giannakis, VUV/Fe(II)/H_2O_2 as a novel integrated process for advanced oxidation of methyl tert-butyl ether (MTBE) in water at neutral pH: process intensification and mechanistic aspects, Water. Res., 166 (2019) 1150–1161.

[54] C.B. Wang, W.X. Zhang, Synthesizing nanoscale iron particles for rapid and complete dechlorination of TCE and PCBs, Environ. Sci. Technol., 31 (1997) 2154–2156.

[55] Y.P. Sun, X.Q. Li, W.X. Zhang, H.P. Wang, A method for the preparation of stable dispersion of zero-valent iron nanoparticles, Colloids Surf., A, 308 (2007) 60–66.

[56] Y.P. Sun, X.Q. Li, J. Cao, W.X. Zhang, H.P. Wang, Characterization of zero-valent iron nanoparticles, Adv. Colloid Interface Sci., 120 (2006) 47–56.

[57] G.N. Glavee, K.J. Klabunde, C.M. Sorensen, G.C. Hadjipanayis, Chemistry of borohydride reduction of iron(II) and iron(III) ions in aqueous and nonaqueous media. Formation of nanoscale Fe, FeB, and Fe2B powders, Inorg. Chem., 34 (1995) 28–35.

[58] H.Y. Shu, M.C. Chang, C.C. Chen, P.E. Chen, Using resin supported nano zero-valent iron particles for decoloration of Acid Blue 113 azo dye solution, J. Hazard. Mater., 184 (2010) 499–505.

[59] A. Eslami, S. Nasseri, B. Yadollahi, A. Mesdaghinia, F. Vaezi, R. Nabizadeh, Removal of methyl tert-butyl ether (MTBE) from contaminated water by photocatalytic process, Iran. J. Public Health, 38 (2009) 18–26.

[60] F.S. dos Santos, F.R. Lago, L. Yokoyama, F.V. Fonseca, Synthesis and characterization of zero-valent iron nanoparticles supported on SBA-15, J. Mater. Res. Technol., 6 (2017) 178–183.

[61] G. Vilardi, D. Sebastiani, S. Miliziano, N. Verdone, L. Di Palma, Heterogeneous nZVI-induced Fenton oxidation process to enhance biodegradability of excavation by-products, Chem. Eng. J., 335 (2018) 309–320.

[62] J.A. Bergendahl, T.P. Thies, Fenton's oxidation of MTBE with zero-valent iron, Water Res., 38 (2004) 327–334.

[63] M. Bertelli, E. Selli, Kinetic analysis on the combined use of photocatalysis, H_2O_2 photolysis, and sonolysis in the degradation of methyl tert-butyl ether, Appl. Catal., B, 52 (2004) 205–212.

[64] F. Fu, D.D. Dionysiou, H. Liu, The use of zero-valent iron for groundwater remediation and wastewater treatment: a review, J. Hazard. Mater., 267 (2014) 194–205.

[65] S. Karthikeyan, A. Titus, A. Gnanamani, A.B. Mandal, G. Sekaran, Treatment of textile wastewater by homogeneous and heterogeneous Fenton oxidation processes, Desalination, 281 (2011) 438–445.